3.4 Reactor Internals Samples

Reactor internals samples were used in both the parametric and laboratory tests. PNNL had acquired the welded stainless steel samples with implanted cracks and notches in 1997. These samples were made for and used in a parametric study and blind test to determine the effectiveness of ultrasonic techniques in finding cracks through welds in austenitic material. These samples were designed to simulate the materials, cracks, and surface conditions common to reactor internals components; i.e., to mock-up a BWR core shroud. The samples consist of approximately 250-mm by 450-mm, 50-mm-thick (10 × 18 × 2 in.) stainless steel slabs that have been cut into two pieces along the center and then welded back together again.

The surfaces of both sides of the samples were machined after welding and crack implantation to smooth them for ultrasonic examination. This machining has hidden all traces of the weld crown in most samples except where the weld crowns were left in the as-welded condition. The samples were machined using the end milling process after welding and crack implantation with a surface finish of roughly 1.6 μm RMS (63 micro-inches). Some samples have also been roughly ground near the weld line and have a surface roughness of at least 12.5 μm RMS (500 micro-inches). Two of the internals samples are shown in Figure 3.5.

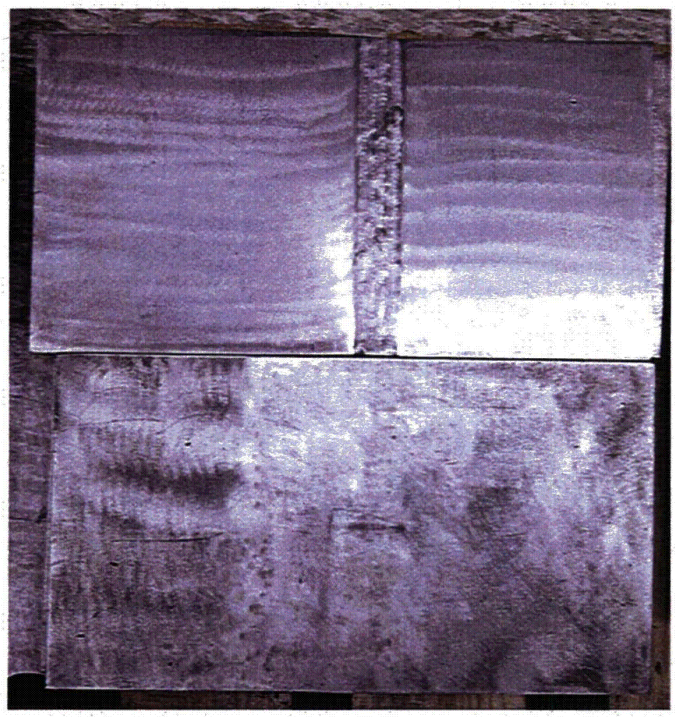

Figure 3.5 Reactor Internals Samples Used in Testing. Top shows weld crown present; bottom shows weld crown removed.

The flaws were implanted into the heat-affected zones of the welds. The flaws were generated by thermal cycling of a tension specimen to produce fatigue cracks of a specific size, removing the crack coupon from the tension bar, then in-situ fusing these coupons during the girth welding process. This technique allows the flaw face to be characterized via precise mechanical measurements and photographs prior to implantation and has been shown to produce cracks in the as-welded condition within ±1.0 mm (0.040 in.) of the specified length and height in the material. Also, this technique enables the vendor to produce various geometrical and welding conditions that simulate those found during field welding; for example, counterbore, inner diameter mismatch, weld root, fusion anomalies, and weld crown configurations.

Normally, cracks implanted in this fashion are not useful for visual testing, as the welding process often causes the two halves to shift in position slightly. This mismatch causes a vertical shift across the two halves of the crack. Odd circumstances can occur such as one lip of the crack jutting over the crack opening, completely covering the crack. Other issues involve the shadows and reflections, caused by lighting a vertically mismatched crack from different angles that are not representative of cracks in the field. Fortunately, the machining process applied to the samples after welding has evened out the surfaces, making the cracks much more representative of cracks expected in the field. It should be noted that effects of deposits or discoloration was not studied in these laboratory tests.

PNNL measured the widths of the cracks in the reactor internals samples using an optical micrometer. This micrometer has a magnification of 100X and a graduated reticule that gives measurements accurately to 12.7 μm (0.0005 in.). The cracks are in general very tight, but there is a good range of crack CODs. The CODs range from less than 5 μm to 125 μm (0.0002 to 0.005 in.) in size. The average COD is 60 μm, (0.0024 in.), with a median crack size of 25 μm (0.001 in.).

For the parametric study, the reactor internals samples were examined in the as-received condition, which contained machine marks and grinding marks, using the three lighting systems. Nine of the samples were then polished and re-examined using the three lighting systems. Scratches were made on the surfaces using 240-grit sandpaper perpendicular and parallel to the crack and were examined with the three lighting conditions at each step.

3.5 Laboratory Tests of Radiation-Hardened Cameras

Two cameras were used for the laboratory tests, a radiation-hardened fixed-focus video camera and a radiation-hardened zoom video camera. Both cameras were black and white only. The two cameras are shown in Figure 3.6.

The fixed-focus video camera has a focal length of 16 mm (0.63 in.) and provided 500 lines of TV resolution. This camera is very strongly radiation-hardened and can be used to inspect recently burned fuel pins in a reactor. The fixed focal length camera is typically used with a pair of spotlights mounted 180 degrees from each other on either side of the lens and can pass the standard 12-μm (0.0005-in.) wire test at a distance of 178 mm (7 in.) in air.

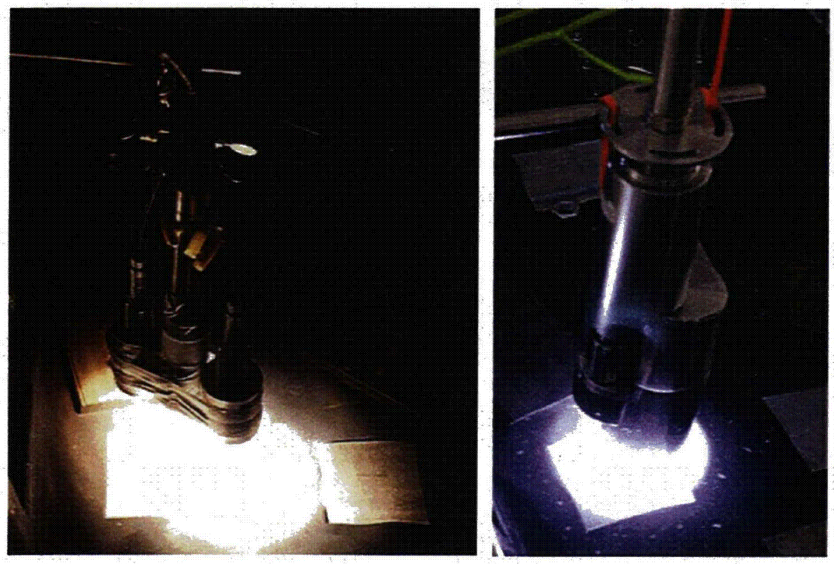

Figure 3.6 Cameras Used for Laboratory Tests. Left: fixed focal length camera with illumination provided by two spotlights. Right: pan/tilt/zoom camera illuminated by LED ring light.

The second camera used was a radiation-hardened video camera on a pan/tilt/zoom head. The pan/tilt/zoom camera uses a CCD imager instead of a video tube and has a zoom lens with a focal length ranging from 8–24 mm (0.31–0.94 in.). The pan/tilt/zoom camera has an integral ring light and provides an image with 470 TV lines. The cameras were mounted on a magnetic track scanner to allow for precise and stable camera movement.

Thirteen cracked and seven blank reactor internals specimens, described in Section 3.3, were placed in random order with random (0 degrees or 90 degrees) orientations inside four long water tanks. The samples were covered in plastic sheeting with thirty 100-mm by 100-mm (4 in. × 4 in.) square windows cut into the plastic. This arrangement provided 17 windows with cracks (some of the internals specimens have two cracks) and 13 windows as blanks. The tanks were filled with water approximately 200 mm (7.5 in.) above the surface of the samples to simulate some of the conditions for performing visual examinations underwater in the field. The test arrangement is shown in Figure 3.7. Photographs of each window are given in Appendix A.

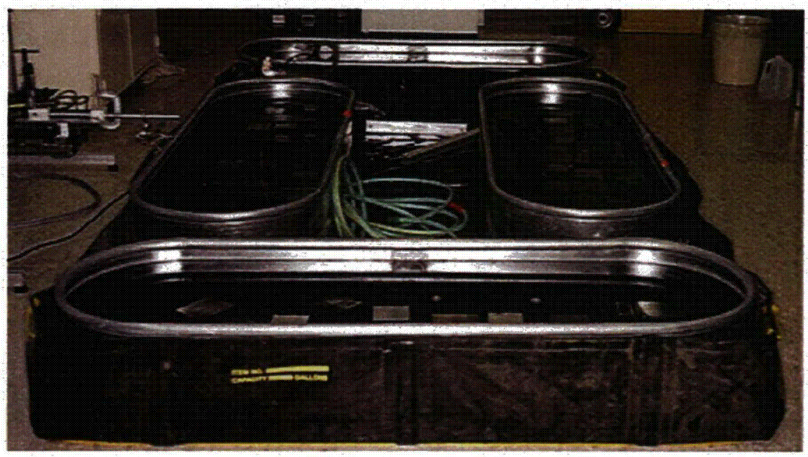

Figure 3.7 Water Tanks with Specimens Prepared for Visual Inspection

Four inspectors were used for the test. Two of the inspectors were PNNL staff with visual testing training. One PNNL staff member is a current American Society of Nondestructive Testing (ASNT) Visual Testing Level III inspector, and the second was previously certified to ASNT Level II but is not currently certified. The other two inspectors were American Welding Society (AWS)-certified visual inspectors contracted through a local company.

The tests were invigilated by a PNNL staff member who had knowledge of the locations and appearances of the cracks used in the study. The PNNL member was able to determine if a call made by an inspector was correct or incorrect and this was noted as each call was made. While ideally such a test would be performed in a double blind fashion, it was decided that the person grading the test should be present during the inspection. This level of grading was needed, so when an inspector made a call the grader was able to ask the inspector to locate the crack on the screen. If the inspector pointed to the crack, the grader noted this as a hit. If the inspector was over a cracked window but indicated a scratch or some other non-crack, the grader noted this as a false call.

4 Parametric Study of Crack Detection Using Visual Testing

PNNL conducted a study on the effects of various parameters on the ability of a mechanical system to image cracks on a stainless steel surface. This section describes the results of the large parametric matrix experiment performed to explore the interaction of crack size, lighting conditions, and surface conditions. Six parameters—crack size, lighting conditions, scanning speed, camera resolution, surface specularity, and surface conditions—were classified according to those over which the inspector has control and those parameters that are sample-dependent. The results for each of these parameters are then described.

4.1 Parametric Matrix Results

The interplay between lighting technique, surface conditions, and crack CODs were explored in a matrix of 192 examinations. This matrix was constructed using nine samples with six CODs, four surface conditions, and six lighting conditions. Each sample was examined in the following conditions: as-received, polished, and with scratches perpendicular and parallel to the cracks. All examinations were performed at the same magnification and with the same resolution setting, 1.3 megapixels.

The most rigorous method of testing each of the inspections would be to have a series of inspectors make calls on the cracked surfaces for each inspection condition. This would be impractical for the number of conditions examined, however. A subjective evaluation was made by one inspector for each condition and the results tabulated. The inspector gave four levels of crack detectability—excellent, good, fair, and poor. This matrix is designed to show general trends for crack detection to help gain an understanding of the complexities of the interactions between and among crack size, surface conditions, and lighting technique.

The results for the subjective evaluation are given in Table 4.1. The results have been color-coded to make the table easier to read. Images of each sample are given in Appendix B. This matrix includes a mix of sample and inspection-dependent variables, and the results will be used throughout Section 4.

Table 4.1 Subjective Evaluation Results for Parametric Matrix for Samples 1-9

Sample 1 – COD 10 microns

Surface Conditions	Diffuse On-Axis	Diffuse Ring	Top Right Spotlighting	Top Left Spotlighting	Horizontal Lighting	Vertical Lighting
As-Received	good	good	poor	poor	poor	poor
Polished	excellent	poor	poor	poor	poor	poor
Parallel	poor	poor	poor	poor	poor	poor
Perpendicular	good	poor	fair	fair	good	good

Table 4.1 (continued)

Sample 2 – COD 10 microns

Surface Conditions	Diffuse On-Axis	Diffuse Ring	Top Right Spotlighting	Top Left Spotlighting	Horizontal Lighting	Vertical Lighting
As-Received	fair	poor	poor	poor	poor	poor
Polished	good	fair	poor	poor	poor	poor
Parallel	poor	poor	poor	poor	poor	poor
Perpendicular	fair	poor	poor	poor	good	poor

Sample 3 – COD 35 microns

Surface Conditions	Diffuse On-Axis	Diffuse Ring	Top Right Spotlighting	Top Left Spotlighting	Horizontal Lighting	Vertical Lighting
Polished	excellent	fair	excellent	excellent	excellent	fair
Parallel	fair	poor	excellent	fair	good	poor
Perpendicular	excellent	poor	good	good	fair	good

Sample 4 – COD 40 microns

Surface Conditions	Diffuse On-Axis	Diffuse Ring	Top Right Spotlighting	Top Left Spotlighting	Horizontal Lighting	Vertical Lighting
Polished	excellent	poor	excellent	good	good	poor
Parallel	poor	poor	good	fair	poor	poor
Perpendicular	fair	poor	excellent	excellent	good	good

Sample 5 – COD 40 microns

Surface Conditions	Diffuse On-Axis	Diffuse Ring	Top Right Spotlighting	Top Left Spotlighting	Horizontal Lighting	Vertical Lighting
Perpendicular	good	fair	poor	good	poor	poor
Perpendicular	excellent	poor	excellent	excellent	excellent	excellent

Sample 6 – COD 50 microns

Surface Conditions	Diffuse On-Axis	Diffuse Ring	Top Right Spotlighting	Top Left Spotlighting	Horizontal Lighting	Vertical Lighting
As-Received	fair	poor	poor	poor	poor	poor
Polished	excellent	excellent	fair	excellent	good	fair
Parallel	excellent	good	good	poor	good	poor
Perpendicular	excellent	excellent	good	poor	good	good

Sample 7 – COD 10-75 microns

Surface Conditions	Diffuse On-Axis	Diffuse Ring	Top Right Spotlighting	Top Left Spotlighting	Horizontal Lighting	Vertical Lighting
As-Received	good	good	fair	poor	poor	poor
Polished	excellent	excellent	poor	poor	poor	poor
Parallel	excellent	excellent	fair	poor	fair	fair
Perpendicular	excellent	fair	good	good	good	good

Table 4.1 (continued)

Sample 8 – COD 125 microns

Surface Conditions	Diffuse On-Axis	Diffuse Ring	Top Right Spotlighting	Top Left Spotlighting	Horizontal Lighting	Vertical Lighting
As-Received	fair	poor	poor	poor	poor	poor
Polished	excellent	excellent	excellent	excellent	excellent	good
Parallel	excellent	excellent	excellent	excellent	excellent	fair
Perpendicular	excellent	excellent	poor	good	excellent	fair

Sample 9 – COD 125 microns

Surface Conditions	Diffuse On-Axis	Diffuse Ring	Top Right Spotlighting	Top Left Spotlighting	Horizontal Lighting	Vertical Lighting
As-Received	fair	fair	poor	poor	poor	poor
Polished	excellent	excellent	good	excellent	excellent	excellent
Parallel	excellent	excellent	good	good	good	poor
Perpendicular	excellent	excellent	good	good	excellent	fair

4.2 Inspection-Dependent Parameters

The following parameters are ones over which an inspecting agency would have control. The choice of camera resolution and lighting style would be made at the time of camera purchase, and the scanning speed would be determined at the time of inspection.

4.2.1 Camera Resolution/Magnification

An important parameter in crack detection is the projected size of each pixel on the imaging chip or the projected width of each TV line in a video tube. Two factors determine the size of the pixel or video line—the number of pixels/lines and the area imaged by the lens. For example, a 640×480 video camera focused on a 75 mm by 50 mm (3 in. × 2 in.) area would have an average pixel size of 117 μm (0.0045 in.). When one may be inspecting for cracks on the order of 10–25 μm (0.0005–0.001 in.), it is clear that inspections are often done with crack sizes lower than or much lower than the size of each pixel. This reduces the contrast and sharpness of the image of the crack as it is averaged into the image of the surrounding metal surface. This situation can be improved either by increasing the magnification or using a higher resolution sensor.

Using high magnification can be very helpful but also carries some serious limitations. First and foremost, inspections carried out at very high magnifications take prohibitively long to conduct. If one wants to inspect an area with a 10-μm pixel size using a standard video camera, one will have to focus on an area 5 mm × 3 mm (0.2 in. × 0.12 in.) in size. Simply put, this is not practical. Second, inspections conducted at very high magnifications tend to rob the inspector of the context of the image. One does not see any fiduciaries in the image for a long time and the inspector can easily become disoriented with respect to location on the component or piece being inspected. High magnification may limit the number of a given crack's branches and bends being imaged on the screen, which may reduce the detectability of the crack.

High-resolution images provide improved contrast between a crack and the background while preserving the benefits of a larger field of view. The primary limitations of high-resolution images are technological. The highest-resolution radiation-hardened cameras have 640 × 480 pixels, and very few monitors have more than 1600 × 1200 pixels. There are six-megapixel video cameras available for machine-vision applications and five-megapixel medical display monitors, but none of this technology has been modified for use in the nuclear industry. It should be noted that viewing a high-megapixel video stream on a lower-resolution monitor can negate the benefit of the high-resolution video stream during a real-time visual inspection. The same crack illuminated under diffuse axial lighting at two resolutions is shown in Figures 4.1 and 4.2. Figure 4.1 shows the area imaged using 1.3 megapixels, and Figure 4.2 shows the same area imaged by the same camera using normal video resolution (640 × 480 pixels). The areas in the images have been cropped to allow the crack to be visible when reduced to fit the margins of this report and do not represent the entire image. The higher-resolution image clearly provides better contrast and detail and superior crack detection. The grayscale level difference between the crack and the background ranges from 10 to 60 levels in the high-resolution image and from only 0 to 20 levels in the low-resolution image. The low-contrast image in Figure 4.2 makes the crack challenging to detect if one does not know its exact location.

Resolution and magnification are secondary to lighting techniques in importance, however. A very high-resolution image with glare and poor contrast between indications of interest and the background is less useful than a lower-resolution image with even, diffuse lighting. The same crack and area imaged at high resolution using a bare-bulb spotlight is shown in Figure 4.3. The grayscale difference is essentially zero between the crack and the background, and while there is no signal from the crack present in the image, the scratches are highlighted very strongly.

4.2.2 Lighting Style

Lighting style can strongly affect all three factors in crack detection. Three lighting styles were used in the parametric study—bare-bulb LED and incandescent spotlights, a diffuse ring light, and a diffuse on-axis light. Examples of a crack illuminated with each technique using the Lightwise 1.3-megapixel video camera are given in Figure 4.4. In each figure, a 12-μm (0.0005-in.) COD crack is in the center of the image with a wire 25 μm (0.001 in.) wide stretched across the image. The metal surface was somewhat specular with some shallow scratches at roughly 45 degrees to the crack and some deeper scratches in line with the crack.

The results from the parametric matrix are shown in Table 4.2. The results show that the diffuse on-axis light provides the best lighting for crack detection. Surprisingly, the spotlighting was comparable to the diffuse ring lighting. While the ring light is somewhat better, spotlights from several directions is comparable. If one can get the spotlights parallel to the crack, one can get better illumination than with the ring light; but when the spotlighting is perpendicular to the crack, the lighting is relatively ineffective.

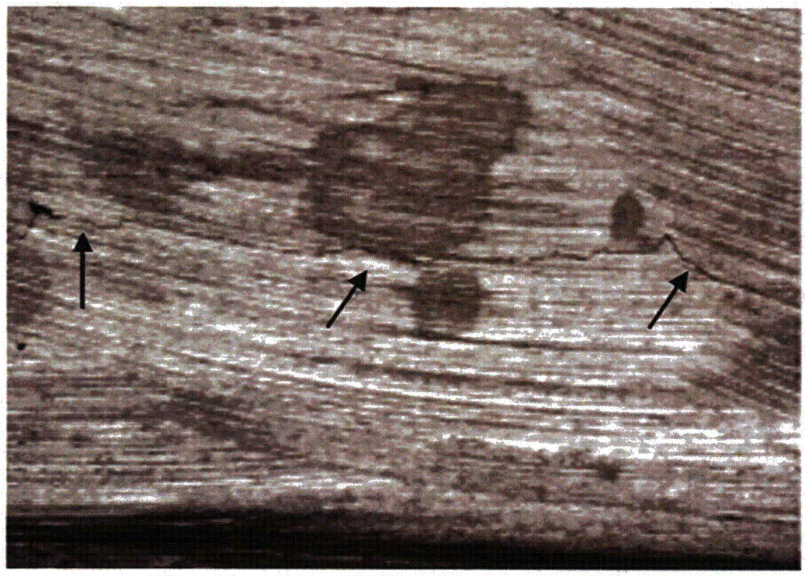

Figure 4.1 12-μm (0.0005-in.) COD Crack Illuminated with Diffuse On-Axis Lighting Imaged Using a 1.3-Megapixel Video Camera Set to Full Magnification. The crack is indicated with arrows.

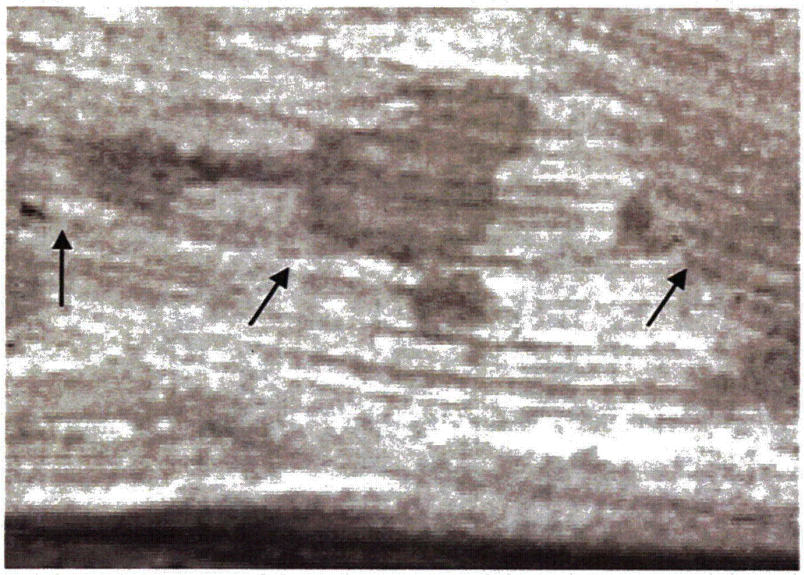

Figure 4.2 12-μm (0.0005-in.) COD Crack Illuminated with Diffuse On-Axis Lighting Imaged Using 640 × 480 Pixels of Resolution. The crack is indicated with arrows.

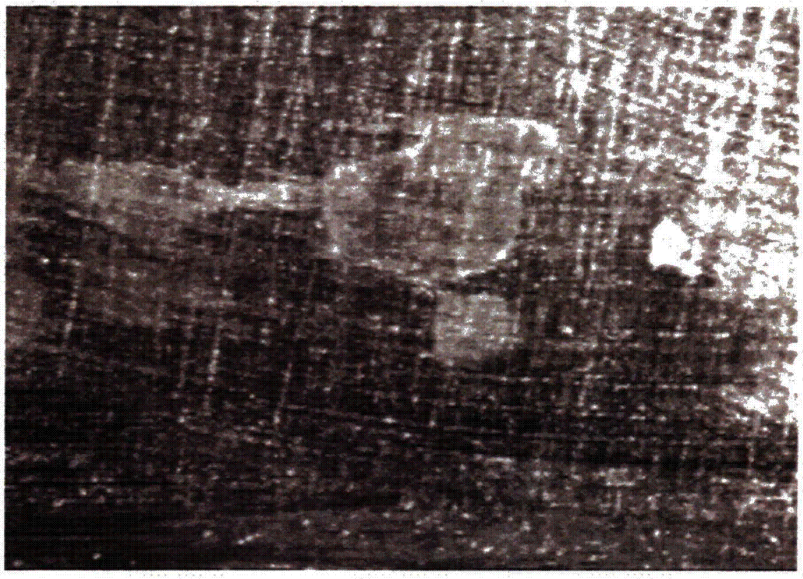

Figure 4.3 12-μm (0.0005-in.) COD Crack Illuminated with Spotlight Imaged Using 1.3-Megapixel Video Camera Set to Full Magnification. In this image, the spotlighting obscures the crack completely.

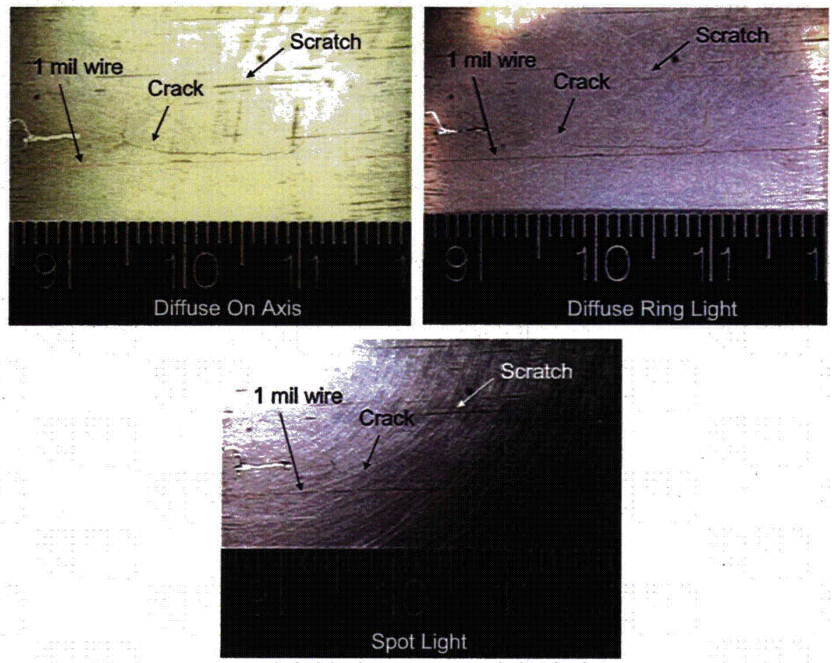

Figure 4.4 Images of Crack, Wire, and Scratches Taken Using Diffuse On-Axis Light, Diffuse Ring Light, and Bare-Bulb LED Spotlight

Table 4.2 Matrix Results for Lighting Techniques

Lighting Style	Excellent	Good	Fair	Poor
Diffuse Axis	56.7%	13.3%	23.3%	6.7%
Diffuse Ring	33.3%	6.7%	16.7%	43.3%
Spot Average	18.0%	25.8%	11.7%	44.5%
Parallel	21.9%	31.3%	6.3%	40.6%
Perpendicular	6.3%	18.8%	18.8%	56.3%
Diagonal Lighting	21.9%	23.4%	10.9%	43.8%

It was determined that spotlighting can be very hit or miss. If the spotlights are arranged perfectly, they can provide good illumination and allow for good crack detection. If the spotlights are aligned incorrectly, they can hide cracks and emphasize scratches and machine marks. Spotlights provided the most glare and most uneven lighting among the three techniques used in this study.

The ring light provides, on average, little glare and good contrast between cracks and the metal surface. The lighting is even across the imaged area, with some weak hot spots but nothing that obscures the image. Shallow scratches and machine marks are somewhat emphasized but are not as pronounced as in the spot-lit images.

The diffuse on-axis light produced a very strong contrast between the crack and the metal background and does not highlight the shallow scratches. The deeper scratches are visible but are clearly discernable as scratches and not cracks.

Poor lighting can cause a very strong drop in visual acuity, even with a very large crack. An example of a large crack (125 μm or 0.005 in.) imaged first using a ring light and then with two spotlights is shown in Figure 4.5. In the image lit by the ring light, the crack is clearly visible as a dark indication. In the spotlight-lit image, the spotlights are perpendicular to the crack, and this lighting does a very effective job of hiding the crack.

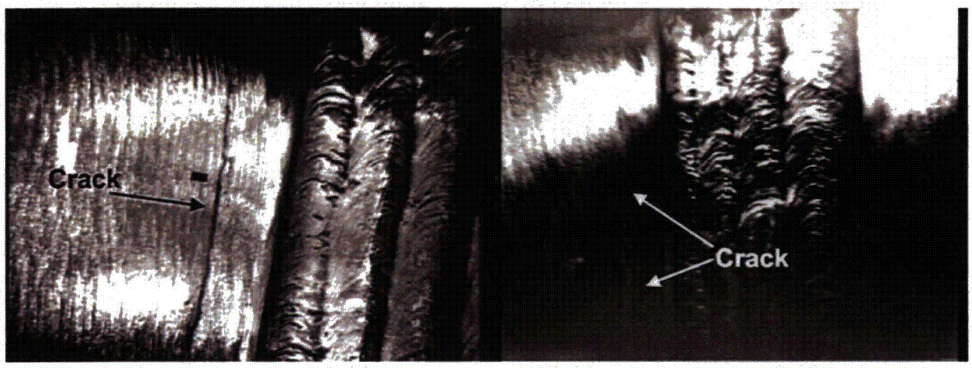

Figure 4.5 125-μm COD Crack Imaged Using Ring Light (left image) and Two Spotlights (right image)

4.2.3 Scanning Speed

The effects of scanning need to be quantified for the actual inspection conditions. Every camera is different, and how a given camera will respond to scanning speed is very strongly dependent on several factors.

When describing camera motion, defining the camera speed is complex. The effects of camera motion on image sharpness are a function of the camera speed, the distance between the camera and the subject, the focal length of the lens, and the exposure time used to take the image. When one is taking images from a moving automobile, objects close to the car can be very blurred while objects very far away would remain sharp. For a digital camera, the ultimate arbiter of the effect of camera motion is the distance a pixel is scanned over the course of the exposure.

Scanning over a surface can have effects on both the contrast and the resolution of the image captured by a camera. The loss of contrast and resolution are caused by the pixel imaging a larger area than it would in a stationary image. The area imaged by each pixel, and the resulting loss in contrast and resolution, increase as the scanning speed and exposure time increases. A specialized system using short-duration flashes and extremely short exposure times can make high-contrast, high-resolution images of a bullet in flight. A video camera in low light produces noticeable loss of acuity when moved even at slow speeds.

The Lightwise video camera was not a good instrument for this test. The refresh rates were very long under typical lighting conditions using the Navitar lens, and any movement tended to completely blur the image. The scanning speed tests were conducted using the pan/tilt/zoom, radiation-hardened video camera used in the laboratory tests.

The radiation-hardened pan/tilt/zoom camera was scanned at speeds ranging from 6 mm/s to 76 mm/s (0.24 to 3.0 in./s) over a 125-μm (0.005 in.) COD crack, and the resulting images were examined. Example images from this experiment are given in Figure 4.6. Slow scanning appeared to cause little distortion in the image, while scanning at 76 mm/s caused gross distortion in the image. The grayscale level contrast between the crack and the background was determined for each scanning speed and compared to a still image of the crack taken using the same camera. The results of the grayscale level calculations are given in Figure 4.7. This experiment shows that at slow speeds the contrast drops slightly, and at higher scanning speeds the contrast drops to less than half of the value of a still camera.

For the resolution tests, the camera was scanned over a 1951 Air Force resolution target, and the camera resolution was recorded for each pass. The smallest resolvable group and element number were recorded, as well as the corresponding number of lines per millimeter. The theoretical maximum resolution for the magnification was 4.7 lp/mm, which is close to the 4 lp/mm that was obtained on a stationary target. Sample images from the scanning speed experiment are given in Figure 4.8. A graph of the results of the scanning speed versus resolution experiment is given in Figure 4.9. It must be stressed that these results are for a given radiation-hardened camera under one set of conditions, but the results for another camera under other conditions may be different.

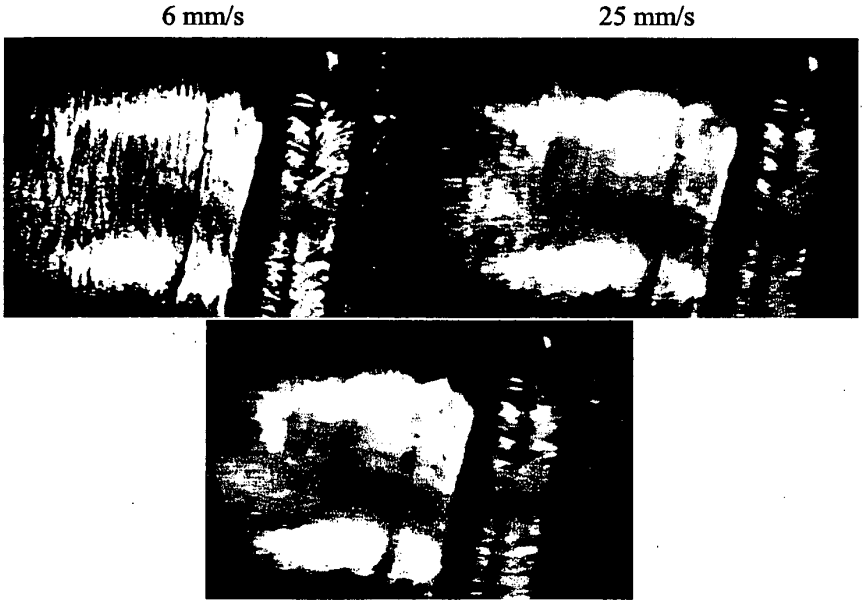

Figure 4.6 Sample Images of a 125-mm COD Crack Imaged at Three Scanning Speeds

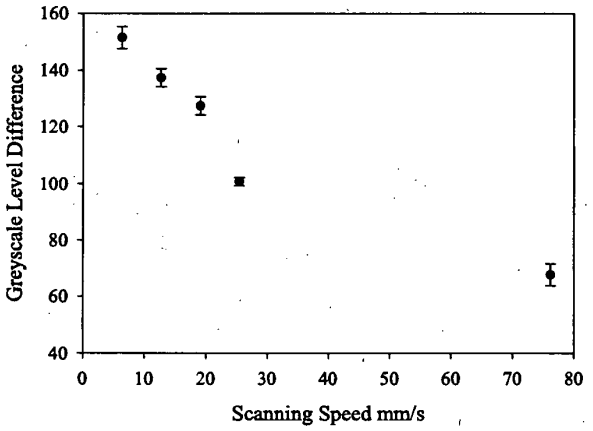

Figure 4.7 Effect of Scanning Speed on Grayscale Level Contrast Between Crack and Background

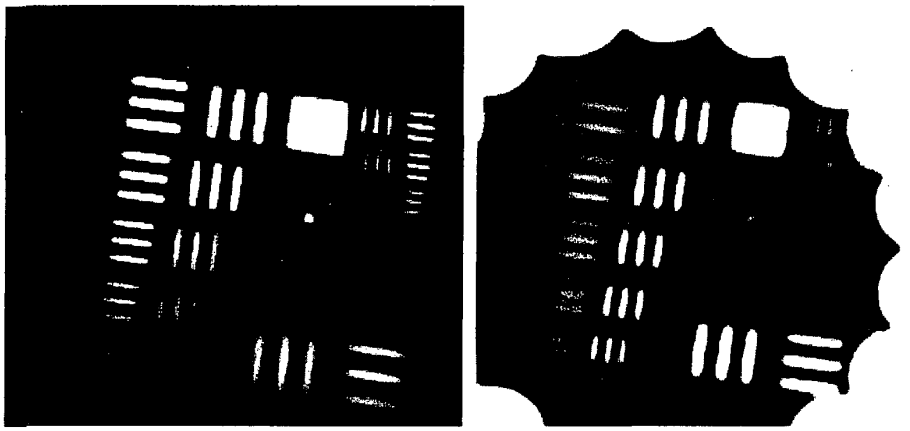

Figure 4.8 1951 Air Force Resolution Target Imaged at Two Scan Speeds

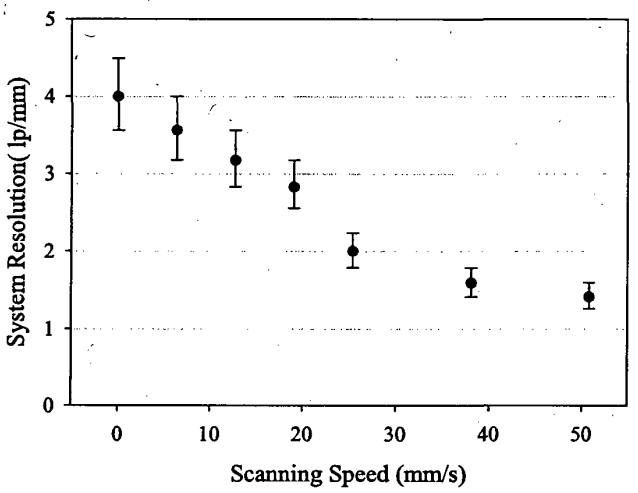

Figure 4.9 Effects of Scanning Speed on Resolution of Radiation-Hardened Camera

The scanning experiment shows that the resolution loss at slow speeds such as 6 mm/s (0.24 in.) do not greatly reduce the resolution of the system, while scanning at higher speeds reduces the resolution to less than half the acuity of a stationary camera.

A factor more difficult to quantify but noted during the test of the effects of scanning was that slow scanning seemed to help the inspectors find cracks. The inspectors reported that the slow scanning gave them the opportunity to view the area of interest from different angles as the camera scanned across and past the area.

As slow scanning (less than 6 mm/s) degrades image quality only slightly and may actually help slightly in crack detection, scanning at these speeds is unlikely to harm the inspection. However, scanning at greater than 25 mm/s (1 in./s) severely degrades the image quality.

4.3 Subject-Dependent Parameters

Although an inspector has a great deal of control over a visual inspection, there are many sample-dependent factors. These factors will be different for each individual component in a reactor. The three subject-dependent parameters examined include the crack COD, the degree of surface scratching, and the surface specularity.

4.3.1 Crack Opening Displacement/Crack Size

As the COD increases, all three main parameters, contrast, recognition, and discrimination between the crack and innocuous features, are improved. The COD affects primarily the contrast between the crack and the background when one is using brightfield lighting. In almost all cases, the contrast between the crack and the background increases as the crack COD increases. Also, the crack becomes more easily recognized as a crack as it gets larger. Crack tortuosity and possible branching are often easier to recognize. Finally, the crack is much more easily discriminated compared to the surface conditions, such as scratches and machining marks, as the COD increases. When a crack COD is larger than the size of the scratches or geometrical effects, it is less likely to be confused for an innocuous feature.

As crack length increases, the crack becomes easier to detect as the inspector has more length over which to recognize the crack. The contrast between the crack and the background is *not* improved by crack length, however. A short crack with a large COD (<100 μm or <0.004 in.) is easier to detect than a long crack with a very small COD (<20 μm or 0.0008 in.).

The parametric matrix results show a strong effect of the COD on crack detectability, as shown in Table 4.3. Cracks larger than 100 μm (0.004 in.) are usually detectable, while cracks less than 20 μm (0.0008 in.) are usually very difficult to detect. The detectability of the middle range of 20- to 100-μm COD cracks depends strongly on the lighting and surface conditions and does not show any clear trend.

A long crack with a wide COD (≥100 μm) can usually be detected on a bad surface with a low-resolution camera under poor lighting conditions. The only time when such a crack becomes difficult to detect is when one is panning the camera quickly over the cracked area.

Table 4.3 Effects of Crack COD on Crack Detectability

COD (μm)	Excellent	Good	Fair	Poor
<20	2.1%	14.6%	10.4%	72.9%
20–40	31.3%	22.9%	16.7%	29.2%
40–100	22.9%	27.1%	16.7%	33.3%
100+	47.9%	16.7%	12.5%	22.9%

4.3.2 Surface Scratching and Machine Marks

The surface of the inspected material has a strong influence on the ability to detect cracks. A mirror-smooth surface can allow for the detection of very tight cracks while a deeply scratched surface or an irregular surface can make crack detection much more difficult. An improperly lit shiny surface can be next to impossible to properly inspect, while a dull matte-finish surface can be quite easy to inspect. For examples of the effect of surface conditions on crack detectability, Figure 4.10 shows cracks of the same width lit using a diffuse axial light on three very different surfaces.

How strongly the surface conditions affect the inspection is greatly dependent on the lighting style. If one used very flat diffuse lighting, then the surface effects can be greatly mitigated. A crack appears as a dark image on a neutral background, even in the presence of scratches and other features such as weld beads.

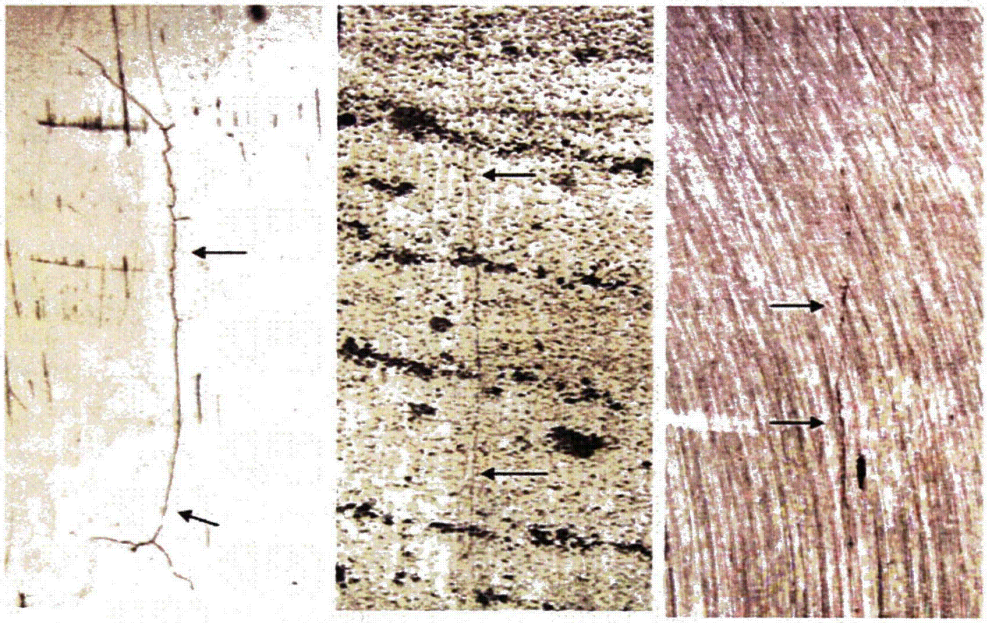

Figure 4.10 Sample Images of Three 12-μm COD Cracks

Poor surface conditions can magnify the effects of poor lighting. A surface with many scratches can become very hard to inspect when one uses spotlighting, for example. As shown in Figure 4.3, poor lighting can greatly emphasize scratches and other marks and obscure otherwise visible cracks.

The matrix results for the effects of surface conditions on crack detection are given in Table 4.4. These show that a very rough surface makes crack detection very difficult. Sample root-mean-square roughness for the samples ranged from 0.0016 to 0.0635 mm (63-250 microinches). A smooth, polished surface yields the best results; when scratching is present, it helps if the scratches are perpendicular to the crack.

Table 4.4 Effects of Surface Conditions on Crack Detectability

Surface Conditions	Excellent	Good	Fair	Poor
Unpolished	0.0%	11.1%	19.4%	69.4%
Polished	45.8%	12.5%	10.4%	31.3%
Parallel	20.4%	18.5%	14.8%	46.3%
Perpendicular	31.5%	35.2%	16.7%	16.7%

4.3.3 Surface Specularity

On the very specular surface of sample 1, the diffuse on-axis light provided the highest contrast between the crack and the background. This light evened out the illumination the most effectively and had negligible glare. The crack appears as a high-contrast dark indication on a bright background. The diffuse ring light provided low glare on the surface, but there were some mixed brightfield and darkfield responses, making the crack image lower contrast than in the diffuse on-axis image. The spotlight provided a darkfield response and is visible against the perpendicular machining marks on the surface. The three images are shown in Figure 4.11.

For a sample with low specularity, the diffuse on-axis light and the ring light provided very similar results, while the spotlight performed very poorly. The crack appeared as a dark indication against a light background in the images made using the diffuse on-axis and ring lights. For the diffuse on-axis light, the contrast between the crack and the background ranges between 20 and 40 levels. For the ring light, the grayscale levels between the crack and the background ranges from 10 to 40. In the image made using the spotlight, the crack is essentially not visible. For most of the crack length, the grayscale level between the crack and the background are the same. At the very top of the sample where the glare is brightest, the grayscale level difference between the crack and the background ranges from 0 to 50. One can find the dark indication against the background if the image is enlarged, but the crack has a much lower contrast than in the other two images. A crack imaged on a low-specularity sample is shown in Figure 4.12.

To ensure that the low-contrast image resulting from the use of the spotlight in Figure 4.3 was not an artifact of using only one lighting angle, the same crack was imaged with the spotlight shining from four angles—from the top, bottom, left, and right of the crack. The results are shown in Figure 4.13. In all images, there is low contrast between the crack and the background. The best contrast is provided by shining light from the right of the crack, which gives a low-contrast darkfield response.

The imaging results for the different surfaces are useful in guiding lighting styles for inspections. If one wishes to inspect a smooth and highly specular surface, one needs to use a diffuse axial light for brightfield imaging or properly angled spotlighting to provide darkfield imaging. For a somewhat specular surface, the ring light and the diffuse axial light perform well, while the spotlight is not especially effective at imaging cracks, even when illuminating from several angles.

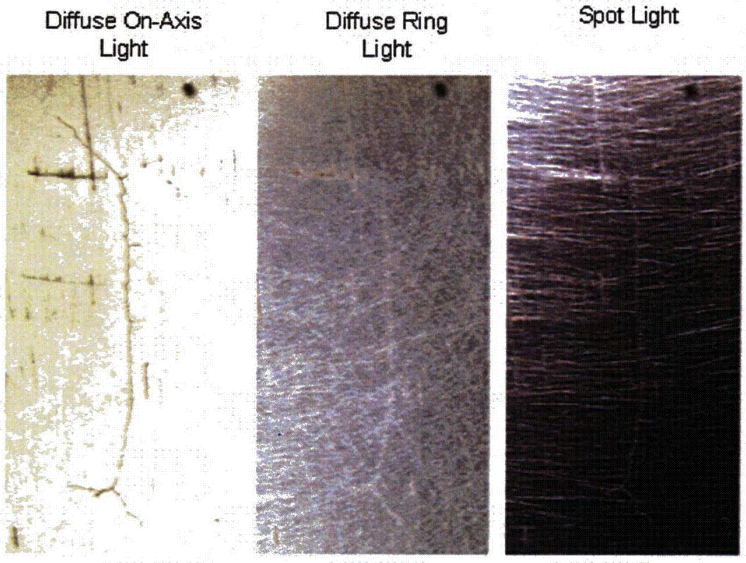

Figure 4.11 Influence of Lighting Style on Crack Detectability on Highly Specular Surface (S/D ratio of 49.86)

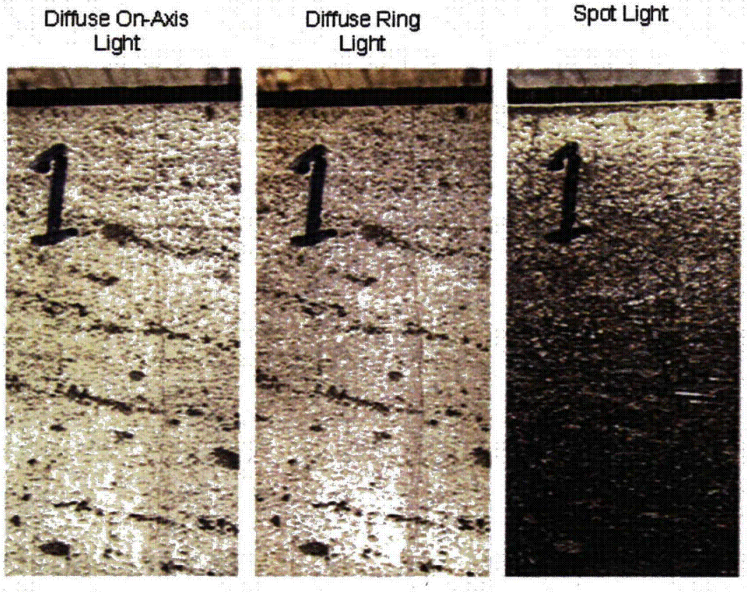

Figure 4.12 Influence of Lighting Style on Crack Detectability on Somewhat Specular Surface (S/D ratio of 4.32)

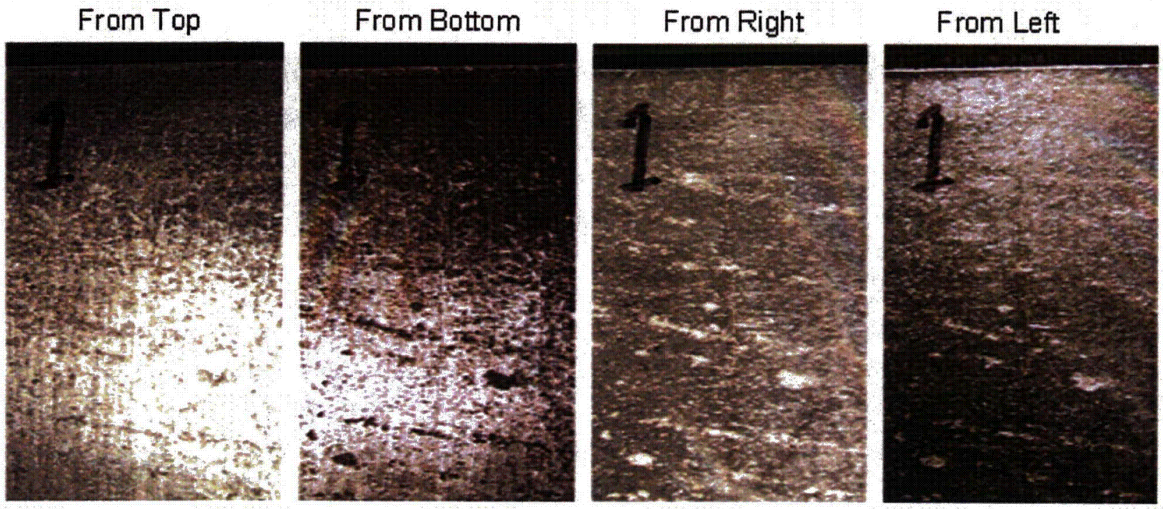

Figure 4.13 Influence of Spotlighting Angle on Crack Detectability on Somewhat Specular Surface (S/D ratio of 4.32)